

VLSI-ENABLED AI-BASED DIGITAL IMAGE PROCESSING FRAMEWORK FOR REAL-TIME RIVER WATER QUALITY ASSESSMENT AND TURBIDITY MONITORING

K.S.SUBHASHINI¹, S. KALYANI², M.K. VARADARAJAN³ and N. KUMARATHARAN⁴

^{1,2,3,4}Dept of ECE, Sri Venkateswara College of Engineering, Sriperumbudur, India

Email to : srinisubha@gmail.com¹, kalsatmah@gmail.com², varadanmk77@gmail.com³, and kumaratharan@rediffmail.com⁴

Abstract

Water quality monitoring plays a crucial role in environmental protection, public health, and sustainable water resource management. Traditional water quality assessment methods often involve labor-intensive sampling procedures, costly laboratory analyses, and delayed result generation. To overcome these limitations, this study proposes a VLSI-enabled artificial intelligence and digital image processing framework for efficient river water quality evaluation, with a primary focus on turbidity estimation and monitoring. Standard turbidity solutions were prepared at 5 NTU intervals and validated using a calibrated nephelometer to establish reference datasets. River water samples were collected from different locations, and high-resolution images were captured under varying illumination and background conditions to analyze environmental influences on image acquisition. Using MATLAB, advanced image processing techniques such as image enhancement, color feature extraction, texture analysis, segmentation, edge detection, and pattern recognition were employed to characterize water quality parameters. Furthermore, the study investigates the integration of Very Large-Scale Integration (VLSI) architectures for accelerating image processing operations and enabling low-power, high-speed implementation suitable for embedded environmental monitoring systems. The extracted image features were compared with standard turbidity references to classify water quality levels accurately. Recent developments in machine learning, computer vision, and VLSI-based hardware acceleration for environmental sensing applications were also explored to enhance monitoring performance. Experimental results indicate that the proposed VLSI-assisted image processing approach provides a rapid, cost-effective, and reliable solution for real-time water quality assessment, demonstrating significant potential for deployment in smart environmental surveillance networks, Internet of Things (IoT)-enabled water management platforms, and next-generation sustainable monitoring systems.

Keywords: Water, image processing, quality, MATLAB software, specimens, sampling, VLSI

1.INTRODUCTION

People started to pay more focus to the ecosystem and preserve the environment as the economic system developed and people's living standards rose. Water, as a life force, has attracted a lot of people's attention. It is extremely significant among all of the leadership, water quality checks, and the appropriate steps against water contamination. Monitoring is much more essential for cloudiness. Many investigations have been reported by scholars in the field

of study, and the results have been positive. Turbidity is a measure of water clarity that synthetically represents all types of contaminants in the water, such as sludge, bacteria, inorganic salts, and so on [1]. Machine vision technology is based on the development of digital images, which are processed using a number of methods and image data is retrieved from the gathered digital images. The information that corresponds to our actual requirement identifies data (like speeding up the picture of the licenceplate license number, implying the present value in the pictures of the tool, and so on) in order to transform image data into the factual data that we require [2]. An convolutional neural network is characterised by the use of a technology to perform various activities in favor of the human brain's output. Unfortunately, there are few fully automated vision-based methods for water pollution identification in the literature that use imaging techniques and a mixture of more than one organic creature. We will present a graphical system that addresses this problem in the following message. It's intended to be a self-contained camera-based groundwater quality inspection system. Our technique has 2 biological organisms that are sensitive to toxins to provide good water quality check results. [4] The first is Lemna minor, an underwater plant with up to 3 leaves on every root. Lemna's main colour is bright green in pristine water without any toxicity, however this colour changes to white and yellow in the presence of toxins. Lemna has a weak immune system to harmful compounds and has a slow reaction time when they are present in a water vessel. The other species has been a well Daphnia magna, a type of water flea. Since its discovery in 1934, Daphnia has been employed extensively in a variety of research. It is a living organism that, like Lemna, has a poor resistance to poisonous compounds but responds quickly to their existence in a tank filled. This distinction is one of the key reasons why the reactions of these 2 organisms to harmful chemicals are coupled to identify a potential potable water concern.

Because machine vision technology takes use of robots to substitute human beings' requirement to experience before even being able to distinguish, it should be classified as advanced systems [5-7]. Neural networks are important in pattern recognition. The diverse patterns in the image recognition system frequently have some regularity characteristics, but these conceptual rules are not linear in most circumstances, thus it is necessary to make a relationship between the model features and classes using a neural network.

CAFOs generate a large volume of wastewater. Reusing cleaned animal manure for barn maintenance and watering can assist incorporate management of water resources substantially [8]. Animal treated wastewater in most CAFOs is confined to open ponds, which are subject to frequent changes in water purity and water retaining capacity. The effluent can contain extra nutrients that are harmful to soil organic growth, as well as chemical pollutants, salts, and viruses that are hazardous to the ecosystem or population health [9]. These dangers can be reduced by closely monitoring if the ponds have provided adequate treatment and whether the sewage has satisfied the crop fields' fertiliser requirements. However, due to a lack of connectivity between CAFOs and water labs, traditional monitoring methods are unable to

offer accurate lagoon water data to enable exact wastewater recycling. As a result, finding a low-cost and efficient lagoon water quality monitoring technology has become a pressing concern. Although there were efforts to improve lagoon monitoring program, these technologies have some expense and generalisability disadvantages. For example,[10] developed an independent water surveillance and testing system that depends on responding automated driving and complicated electrical signal process control to analyse water chemical variables. presented an IoT water tracking system that can monitor water status in real time. The surveillance cost of this system, however, was relatively significant, making the technology ineffective.

[11]created a water purification system using a chemical gas sensor and a virtual instrument approach. However, not only does this system rely on the sample's purity, but the measuring process itself is time demanding.

Image processing has been a prominent analytical tool that has been used in a variety of fields[12]. It has the potential to significantly lower both lab test and labour expenses. [13]. Recent improvements have shown that image processing approaches may be used to evaluate and assess bacteria in wastewater, forecast inflation events, and precisely place flocs[14]. Remote sensing has employed RGB colour coordinates to detect and forecast soil and geologic elements in sparsely vegetated areas. [15],

developed an RGB value sewage monitoring system based on a digital image produced from a specific point of true colour image. The American Dye Manufactures' Institute 3 and 31 wavelength approaches can efficiently measure sewage for true colour and apparent colour as a tristimulus filter by utilising a spectrometer as the measuring system.

2. DESIGN

2.1 Mechanical Design

Two manufacturing cameras are linked to a computer using the Matlab programming environment as well as the Image Collection and Computer Vision Toolbox to provide a technological solution for visual examination. The basic concept behind water quality testing is to fill 2 distinct containers with the same water . place Lemna minor for one vessel and Daphnia magna in the other. Figure 2 shows our experimental workspace, which was set up for a machine vision activity. The first vessel, as previously said, includes any Lemna minor organism that is obviously green and develops broad in a top if water quality are ideal in terms of toxicity. When low-purity water is present, the Lemna minor's hue and surface deteriorate drastically. In a few hours, the Lemna'scolour changes rapidly to yellow or white, although its surface changes relatively minimally. The second application of Daphnia magna was very identical to the first. The only distinction is that Daphnia's life is determined not by its colour or surface, but by the speed with which individual animals move. Simply put, more Daphnia activity means clearer water. Other image processing techniques should be utilised to estimate

the current viability of *Daphnia* species, according to the findings.

The two manufacturing cameras placed above the containers in our design monitor both the *Daphnia*'s and the *Lemna*'s vessels. After a predetermined amount of time has passed, both containers are scanned again. Each image is promptly processed, and the findings are combined with the previous iterations' findings. The only two characteristics retrieved from the photos of the *Lemna* organism are the clarity of green colour and the general surface of green colour. In the instance of *Daphnia magna*, a technique of detecting overall present movement of the present fleas is based on a discrepancy between two photographs in a sequence.



Fig. 3. The color CCD cameras captured a series of two pictures: *Lemna minor* (on the left) and *Daphnia magna* (on the right).

Despite its simplicity, this strategy is surprisingly effective for robust image acquisition devices. B. Image Obtaining Obtaining photos of both species in the vessels is the first stage in the inspection assignment. Two identical Imaging Source Ltd. commercial USB webcams with a size of 1280 by 960 pixels were utilised to achieve this. A manual illumination mode was chosen as a suitable method due to the regular and reliable sequence of obtained images [6]. In the case of *Lemna*, the exhibition time is directly set to 1/20 s for the first image and 1/30 s for the second image. Finally, due to consistent acquisition, the cameras' automated white balancing feature has been disabled. Image segmentation in both the *Lemna minor* and *Daphnia magna* examples is very simple, requiring only basic image processing techniques with straightforward execution [10, 11]. The photographs of *Lemna* are processed using a technique based on colour data in visual information [9], whereas the pictures of *Daphnia* are handled as a series of dynamical pictures and mutual movement is recognised using a differential approach.

2.2. Image Processing And Classification

The Pictures of Lemna Minor Have Been Processed The photographs captured by a camera mounted on top of the container with the Lemna species are in typical Rgb image. Almost all colour commercial cameras have a native format that isn't exactly what we need for the colour analysis that follows. The RGB colour space is converted to an alternate colour space called as a YCbCr in order to accomplish exact and reliable colour research and examination. These 2 colour spaces are virtually identical, with the exception that the Y element of grey levels is expressly specified in the YCbCr format. The conversion from RGB to YCbCr is clear and may be repeated without losing data accuracy. We employed a basic method for categorization of each component of a source images in the instance of Lemna's hue and surface characteristic. The luminance component Y was removed, and an actual set of photos was used to create a prediction algorithm of a healthy Lemna species in the residual CbCr plane. Figure 1 shows an example picture of a normal Lemna species and a corresponding prediction method in the CbCr plane.

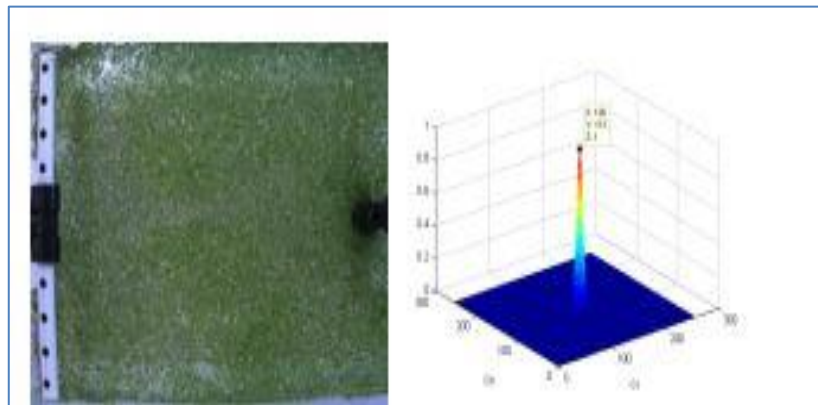


Fig. 1. A healthy Lemna organism and the bayesian classification algorithm (on the left)

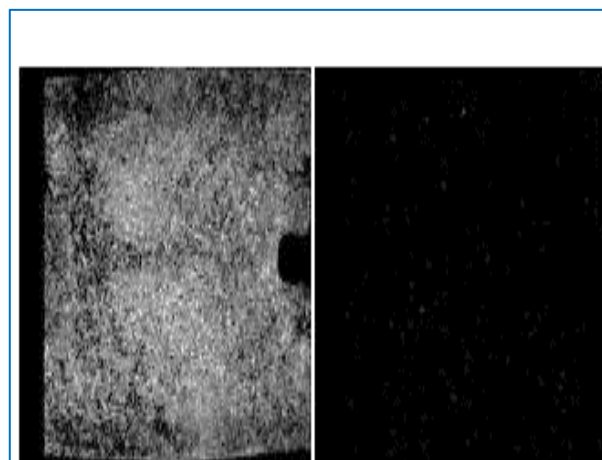


Fig 2: Images of the probability model: probabilistic maps of green and yellow colours on the left and right, respectively. Each combination of input pixel values Cb and Cr

receives a clear response from the model.

This response calculates the probability that a given pixel corresponds to the bright green class. A position in the Lemna class is also associated with this chance. Because the normal Lemna organism was completely green, only the green band of the input image is used in the classification problem. The unhealthy is the inverse of the healthy. The colour of the Lemna organism degrades, notably towards white and yellow, and the Cr component enters the classification phase. As a result, not only is the previously mentioned stochastic map associated to the G generated. The same method is used to create a map connected to the RG, and both images are eventually integrated into a single synoptic image.

As seen in Fig. 2, the probability map associated with the green colour merely reflects how healthy Lemna's species is. The probability map associated with the yellow colour, on the other hand, expresses how hazardous the same creature is. These two classifications, however, do not complement each other. In the colour space, there is a huge gap (called neutral) between the hues of the unhealthy and healthy Lemna. The lack of the Lemna organism or a colour of Lemna other than green or yellow causes the black patches in Fig. 6. The total area of all green items in an image is the single representative characteristic for determining quality of the water as the final step.

The surface of a healthy Lemna was expressed as an integer, which is equivalent to the total of all rgb components within a specific ROI in an image. A graph with a rising, declining, or stable trend is created by a succession of these integers corresponding to successive iterations. The Lemna organism's comparative fitness is then calculated as a proportion of the last and initial samples in the graph.

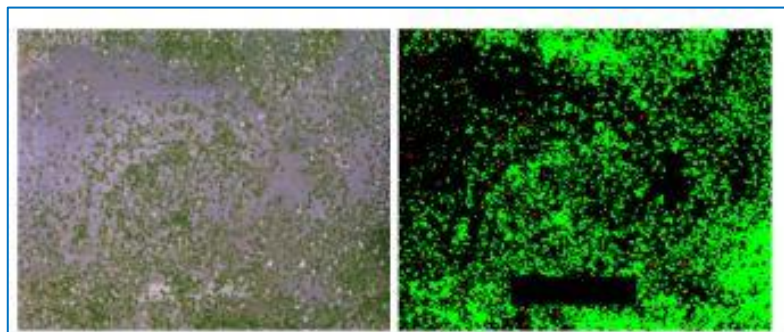


Fig. 3. An example of Lemna's input image with the segmented healthy (G) and unwell (R) items.

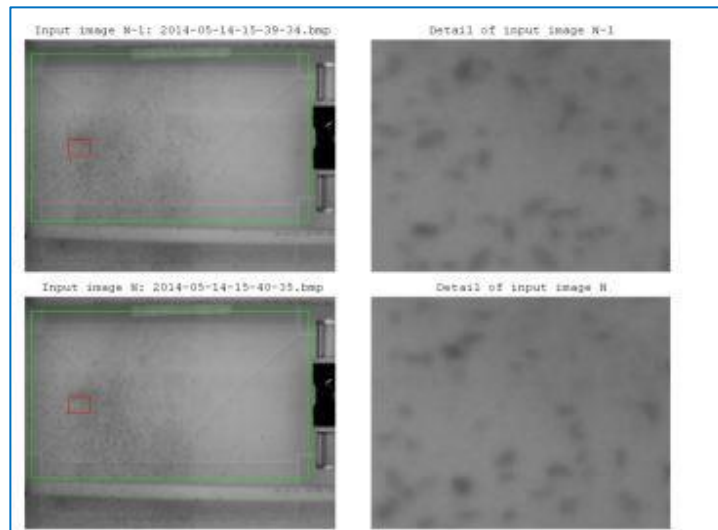


Fig. 4. In the left column, there are a couple of input photographs, and in the right column, there are highlighted details (red rectangles).

From an ecotoxicology standpoint, this fitness feature is closely related to the investigated water cleanliness. Image Analysis of Daphnia Magna A technique for processing photographs of the Daphnia magna is totally different from the color-based method for analyzing images of Lemna minor, as discussed in one of the earlier chapters. Only an exact measure of present mobility activity is required for the purpose of water quality monitoring.

A continuous series of Daphnia organism pictures is obtained and then used as an initial data for image processing techniques. For the identification of present motion activities of Daphnia microorganisms, a so-called differential imaging approach was used. In general, a current picture is deducted from a model, which is also known as a backdrop model. The differential image is created as a result of the subtraction, with bright pixels corresponding to spots in the current source images where values have altered against the models. In the literature, there are numerous methods for determining the model picture.

Following multiple tests, we've chosen to employ a simple reduction of the sequence's two successive photos. If the current picture $IN(x,y)$ has an index of N , the model will be the picture $IN-1(x,y)$ with an index of $N-1$. Because the length traversed by healthy Daphnia creatures between 2 subsequent photos is much more than their average duration, this method can be used. It means that healthy organisms can move enough in the contrast image to be seen. Figure 4 shows examples of two sequential photos with their matching features.

Because we don't wish to recognise individual organisms, it's obvious that subtracting the two sequential photos can be beneficial for estimating current activity. In such circumstances, a

different method for determining the background must be employed. The equation expresses the chosen approach for computing the divergent image $DN(x,y)$ mathematically (1).

$$D_N(x,y) = |I_{N-1}(x,y) - I_N(x,y)| \quad (1)$$

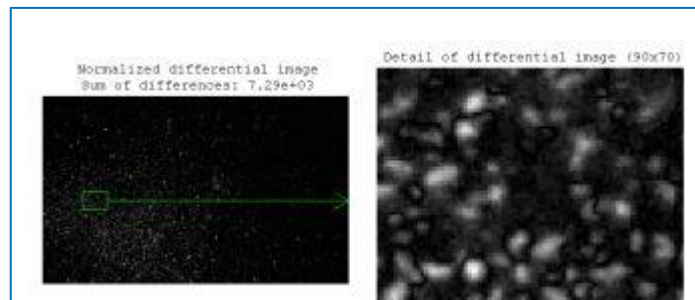


Fig. 5. On the left, a normalised differential image, and on the right, a markedly enhanced detail.

Because the orientation of the organisms' motion is not significant in this assignment, the resultant image numbers of the divergent picture are handled in absolute value, as shown by the the equation. The divergent image was only visible in its normalised form in Fig. 8, but it is used for all calculations in its quasi original state. As previously stated, pixels with high intensity value in the $DN(x,y)$ represent places with large movement, and photons with low intensity value represent static areas with no movement.

The thresholding procedure must be performed in order to obtain a binary image because the generated differential picture is yet a continuous signal with a large number of luminance. The excessive current image $DN(x,y)$ is thresholded with the threshold level of to produce this binary mapping of present disparities. The conventional formula, written here as the equation, then yields the binary map $BN(x,y)$ (2). In each cycle, the criterion of given by formula (3) is adaptively chosen based on the largest value in the present divergent image. During the whole picture series analysis, a continuous sensitivity degree of the thresholding process is maintained.

$$B_N(x,y) = \begin{cases} 0 & |I_{N-1}(x,y) - I_N(x,y)| < \varepsilon \\ 1 & |I_{N-1}(x,y) - I_N(x,y)| \geq \varepsilon \end{cases} \quad (2)$$

$$\varepsilon = f[\max(D_N(x,y))] \quad (3)$$

In Fig. 6, all of the stages of the image analysis approach explained thus far are clearly displayed. The two input pictures I_N and I_{N-1} are in the first row, the relevant differentiated

image DN and its normalised form is in the second row, and the binary mapper BN and the first control signal IN with the underlined differences is in the third row. In the final step of categorization, a scalar value derived from the total of all single variations is merely one indicator for assessing water quality depending on Daphnia organism motion.

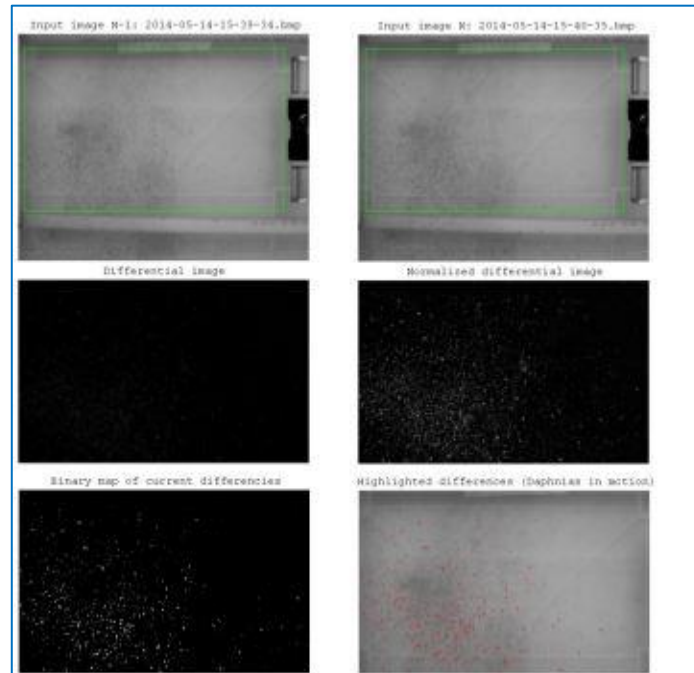


Fig. 6. The binary image BN and marked moving creatures in the original image in the bottom column, the simple divergent image DN and the normalised differential picture in the middle row, and the 2 input images IN and IN-1 in the top row.

As a result, relative engagement levels will inevitably fluctuate more than intended. Furthermore, because the Daphnias' motion is partially unpredictable and unstable, we're interested in tracking relative movement over a longer time. Its waveform must be filtered to prevent the relative activity's shifting shape. Because it allows for easy filtration along the temporal axis, the rolling average method was chosen as a convenient way to achieve this.

$$RA_f(i) = \frac{RA(i) + RA(i-1) + \dots + RA(i-M+1)}{M} \quad (4)$$

where RA(i) represents the value of an initial relative action in the i-th iteration, RAF(i) represents the value of a filtering relative action in the i-th iteration, and M is the width of the rolling average filter. In Fig. 10, the raw numbers of relative activity as well as the filtered data by the rolling average oscillations are shown. An alarm relating to filthy water will occur if the present value of the observed relative action is less than this defined limit. Figure 11 shows two examples of evaluating a whole gallery throughout the course of two days of measurement.

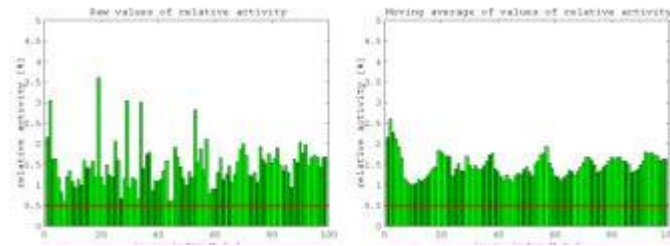


Fig. 7. On the left, the raw comparative activity levels waveform, and on the right, the same sine wave processed by a moving mean filter with a width of $M = 5$.

Both the image capture duration and the breadth of the moving mean filter were set in these two trials.

3. RESULTS

Because these distinct monitoring sections are handled as independent measurements in independent vessels, the findings of the Lemna and Daphnia organisms' procedures have the identical weight and significance for a target application. As a result, if merely one result exceeds the given limit, a global alarm will be triggered. We ran a number of experiments in the open assessment galleries, as well as some strict checks in each of the three possible galleries. Because a similar trend was detected in both situations when the liquid in both vessels was contaminated throughout our studies, the results appear to be excellent. In the instance of Daphnia monitoring, the method outlined takes only absolute differences in luminance between two photos into account.

Noncontextual fragmentation is the name given to this type of image processing operation. In the event of contextual separation, a far more complicated approach for computing or estimating the vessel's reference image will be calculated or projected. As a result, the procedures we employed to assess water unfitness are quite easy and quick to execute. Unfortunately, as previously stated, a non-contextual technique for Daphnia organism motion sensors is extremely limited for future demand and will almost certainly be supplanted by some sort of contextual feature extraction with other features capable of monitoring individual items independently.

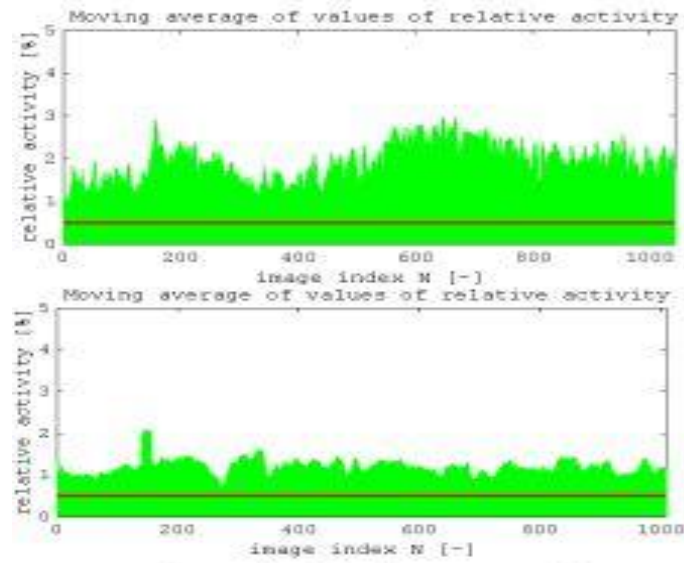


Fig. 8. The two waveforms correspond to two entire one-day galleries filtered by 2 distinct width moving mean filters.

4. CONCLUSIONS

This study demonstrated the effectiveness of a VLSI-enabled digital image processing framework for rapid and reliable river water quality assessment, with a particular emphasis on turbidity monitoring. By utilizing standard turbidity samples validated through nephelometer measurements and analyzing river water images acquired under different environmental conditions, the proposed approach successfully established a correlation between image-based features and water quality characteristics. Advanced MATLAB-based image processing techniques, including feature extraction, segmentation, texture analysis, and classification, proved capable of identifying variations in turbidity levels with high consistency.

The integration of VLSI technology provides a pathway toward high-speed, low-power, and hardware-efficient implementation of image processing algorithms, making the system suitable for real-time environmental monitoring applications. Compared with conventional laboratory-based methods, the proposed framework offers significant advantages in terms of reduced operational cost, faster processing time, portability, and ease of deployment. Furthermore, the incorporation of artificial intelligence and computer vision techniques enhances the automation and accuracy of water quality evaluation.

The findings indicate that VLSI-assisted image processing systems can serve as a practical alternative for continuous river water surveillance and smart water resource management. Future work may focus on integrating IoT-based sensing platforms, deep learning models, and

FPGA/ASIC-based VLSI architectures to enable large-scale, real-time monitoring of multiple water quality parameters, thereby supporting sustainable environmental protection and informed decision-making processes.

REFERENCES

1. Teta, Roberta, et al. "Cyanobacteria as indicators of water quality in Campania coasts, Italy: a monitoring strategy combining remote/proximal sensing and in situ data." *Environmental Research Letters* 12.2 (2017): 024001.
2. Batur, Ersan, and DeryaMaktav. "Assessment of surface water quality by using satellite images fusion based on PCA method in the Lake Gala, Turkey." *IEEE Transactions on Geoscience and Remote Sensing* 57.5 (2018): 2983-2989.
3. Prabakaran K., Vengataasalam S., Balaji G. "Numerical analysis of state space systems using single term Haar wavelet series" *Applied Mathematical Sciences* (2014).
4. Hema, S., Devi, P. S., Alkabbji, R., Lincy, B., Bahl, A., & Karthikeyan, G. (2025, July). Deep Learning in Robotics, Smart Technologies, and Medical Devices Using Very Large Scale Integration (VLSI)-Based Embedded Systems. In *2025 International Conference on Information, Implementation, and Innovation in Technology (I2ITCON)* (pp. 1-6). IEEE.
5. Abirami, G., Arunkumar, T., Raghavendran, N., Maheswari, G. U., Senkumar, M. R., & Saravanakumar, R. (2026, April). VLSI-Enabled Intelligent Access Control with Automated Biometric Authentication. In *2026 Fourth International Conference on Augmented Intelligence and Sustainable Systems (ICAISS)* (pp. 1206-1212). IEEE.
6. Palanikumar, G., Gopal, B., Prasad, S., Jubran, A. M., Bhardwaj, N., & Dinesh, M. (2026, February). Application of AI-VLSI, RFID, Motion Sensors, and a Remote Surveillance System: Identify an Online Fraud Detection for Automated Teller Machines. In *2026 International Conference on Emerging Technologies and Future Innovations (ETFI)* (pp. 1-6). IEEE.
7. Adinath, M., Parvesh, S. M., Abinandhan, R., Aadhitya, S., Seshua Sai, M., & Shamili, E. (2026, February). Design of a VLSI Enabled Quantum-Resistant Blockchain Architecture with AI (Artificial Intelligence)–Driven Intrusion Detection System and Computer Vision for Secure Embedded, Internet of Things Edge Systems. In *2026 1st International Conference on Advancing Sustainable Solutions through Technologies (ICASST)* (pp. 1-6). IEEE.
8. AM, A. B., Agarwal, S., Stephan, P., & Stephan, T. (2024). IoT-Based Automatic Water Quality Monitoring System with Optimized Neural Network. *KSII Transactions on Internet & Information Systems*, 18(1).
9. Pandey, P., Mishra, R., & Chauhan, R. K. (2022). Future prospects in the implementation of a real-time smart water supply management and water quality

- monitoring system. Larhyss Journal, 19(4), 47-61.
10. Kara, S., Karadirek, I. E., Muhammetoglu, A., & Muhammetoglu, H. (2016). Real time monitoring and control in water distribution systems for improving operational efficiency. *Desalination and water treatment*, 57(25), 11506-11519.
 11. Hong, E. M., Choi, J. Y., Nam, W. H., & Kim, J. T. (2016). Decision Support System for the Real-Time Operation and Management of an Agricultural Water Supply. *Irrigation and Drainage*, 65(2), 197-209.
 12. Khatavkar, P., & Mays, L. W. (2020). Real-time operation of water-supply canal systems under limited electrical power and/or water availability. *Journal of Water Resources Planning and Management*, 146(4), 04020012.
 13. Creaco, E., Campisano, A., Fontana, N., Marini, G., Page, P. R., & Walski, T. (2019). Real time control of water distribution networks: A state-of-the-art review. *Water research*, 161, 517-530.
 14. Romano, M., & Kapelan, Z. (2014). Adaptive water demand forecasting for near real-time management of smart water distribution systems. *Environmental Modelling & Software*, 60, 265-276.
 15. Kurtz, W., Lapin, A., Schilling, O. S., Tang, Q., Schiller, E., Braun, T., ... & Brunner, P. (2017). Integrating hydrological modelling, data assimilation and cloud computing for real-time management of water resources. *Environmental modelling & software*, 93, 418-435.